# Advance Materials - Process Optimization, Microstructure and Hardness of Additively Manufactured Co-Cr Aerospace Alloy

**L. O. Osoba, O. A. Ojo**
[1]Department of Metallurgical & Materials Engineering, University of Lagos, Lagos, Nigeria
[2]Department of Mechanical & Manufacturing Engineering, University of Manitoba, Winnipeg Manitoba, R3T 5V6, Canada
Email: losoba@unilag.edu.ng, olanrewaju.ojo@umanitoba.ca

**Abstract**
*In the current study, the effect of carefully designed Powder Bed Fusion (PBF) laser parameters on the microstructure and hardness of Co-Cr alloy straight, thin-wall additively manufactured test coupons that are as-built or have undergone Hot Isostatic Pressing (HIP) was investigated. For enhanced productivity, it is important to evaluate the relationship between energy density (ED) input (laser power, scan speed) and the microstructure developed in the Co-Cr alloy coupons for an aerospace application. Both the High ED and Low ED input processing laser parameters induce a higher percent (%) volume of defects in the as-built coupons when compared to the manufacturer recommended benchmark parameters. However, after HIP, the % volume fraction of defects reduces significantly, and the microstructure is homogenized. Furthermore, the strength of the test coupons manufactured using the manufacturer recommended laser parameters is comparable to those obtained in the low ED input test coupons after HIP; which invariably could be utilized to enhance productivity significantly. In addition, the surface roughness of the Low ED input parameter coupons after HIP is similar to the coupons produced using the manufacturer recommended laser parameters assessed with light optical magnification image evaluation. Hot Isostatic Pressing is therefore an excellent post-processing method to reduce internal defects for a given range of laser energy densities in metal additive manufacturing at increased build speeds.*

**Keywords:** Additive manufacturing, Defect, Hot Isostatic Pressing, Energy Density, Hardness.

## 1.0 INTRODUCTION

Over the last decade, additive manufacturing (AM) technology has consistently evolved as a sophisticated rapid manufacturing tool that allows direct fabrication of an end-usable part with complicated shapes e.g. complex vanes and air ducts that are almost impractical to fabricate by other manufacturing processes. This process involving the sequential addition of ultra-thin layers of material without extensive tooling, has been recognized and predicted as a key tool that will revolutionize manufacturing processes for many industries (Sankaranarayanan *et al.*, 2016).

Although AM, which is also known as 3D printing, has become relatively popular for fabricating parts from plastics, the use of AM to produce metallic components, which faces a much higher level of design challenges and post processing requirements, is expected to have its most commercial impact in aerospace and biomedical applications (Zhang *et al.*, 2006; Williams *et al.*, 2015; Thompson *et al.*, 2015; Syed *et al.*, 2005; Kinsella, 2008). Different techniques are currently being used for AM of metallic products and one of these is the powder bed fusion (PBF) process technology. In this technology, the additive material (powder) is used to produce metallic part directly from 3D model data. PBF can be performed with either laser or electron beam as the thermal source to melt the powder. The process also includes a mechanism to pre-spread a smooth powder layer on the bed and control the powder fusion to a specific region during each layer scan (Choi and Chang, 2005).

Since material properties are inherently controlled by their microstructure, an in-depth understanding of how material microstructure is influenced by AM process parameters is

fundamental to engineer desirable properties by this emerging technology. It has been found that one of the key microstructural features in metallic products produced by powder bed fusion (PBF) and which could have dire detrimental effects on mechanical properties, such as, tensile, fatigue and impact toughness is defects of various form, such as, incomplete melting and porosity (Kim *et al.*, 2017; Asala *et al.*, 2017; Zhong *et al.*, 2015; Gong *et al.*, 2015). Accordingly, an adequate understanding of microstructure in terms of processing parameters variables that can affect defects and pore formations with possible effective measures that can be taken to eliminate and or reduce such defects and porosity are crucial to producing metallic products with reliable properties and performance by the AM technique.

In this current study, laser metal powder bed fusion (PBF) AM method was used to produce thin-wall Co-Cr alloy samples part typically used in aerospace application with the view of evaluating the relationship between energy density (ED) input (laser power, scan speed) and the microstructure developed in the Co-Cr alloy coupons. The objective of this study is to perform systematic microstructural analyses and hardness evaluation on test coupons that are as-built and those that have undergone Hot Isostatic Pressing (HIP). The ultimate goal of this study is to enable a better understanding on the influences of energy density on as-built defects in the Co-Cr alloy and the consequential role of HIP on the as-built defects in order to develop optimal processing parameters that will enhance fabrication of better quality Co-Cr parts by laser metal PBF.

## 2.0 MATERIALS AND METHOD

Carefully designed energy densities process optimization parameters were developed as shown in Table 1, to produce the Co-Cr AM coupons. These included Low energy density parameters, manufacturers' recommended parameters and High energy density parameters. The Co-Cr powder with proprietary chemical composition was sourced from Original Equipment Manufacturer (OEM). Figure 1 shows the design plan and the 3D printing layout plate of the design of experiment. A total of 75 parameters (in duplicate – 150 coupons) were produced in an as-built configuration (Figure 2) and then an identical build was reprinted to undergo Hot Isostatic Pressing (HIP). After production and subsequent HIP of one set (150 coupons), both the as-built and HIP coupons were EDM machined and subjected to one of the oldest, simplest but reliable non-destructive test (NDT) methods, Liquid Penetrant Inspection (LPI) at standard non- destructive laboratory in Winnipeg, Manitoba Canada. Three cross-section image each were capture using a Light Optical Microscope (OM) and Scanning Electron Microscope (SEM) at 200X and 500X magnification respectively from transverse sections across the built (Z) direction of selected coupons. The images from OM and SEM were then converted into de-noised, black-and-white micrographs using Image J porosity analysis software to quantify % volume fraction of internal defects (Figures 3). Micro-hardness tests were performed using a Buehler Micromet 5100 series hardness tester on a load setting of 300 gf and a step size of 0.5 mm. The values of the micro-hardness were determined from an average value of 20 data points

**Table 1. Design of the Experiment**

| Energy Parameters | High | Recommended | Low |
|---|---|---|---|
| **Part Thicknesses (t) (mm)** | 0.0762/0.889/1.016 | 0.0762/0.889/1.016 | 0.0762/0.889/1.016 |
| **Stripe Scan Power (P) (Watts)** | | 245 – 145 | |
| **Stripe Scan Speed (V) (mm/s)** | | 1200 – 400 | |
| **Energy Densities (P/V)** | 2.26 | 1.01 | 0.59 |

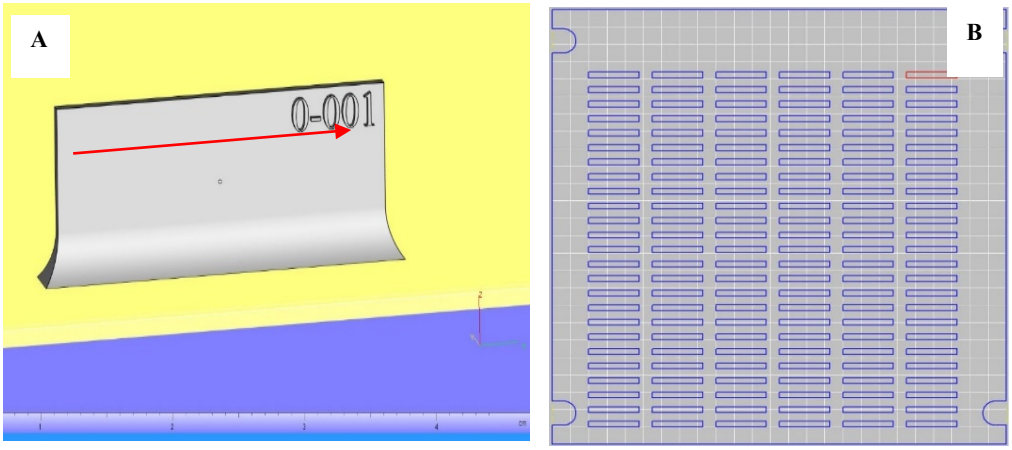


**Figure 1: (A) typical coupon design with an identification mark (arrow show the scanning direction), and (B) shows the built plate design/layout**

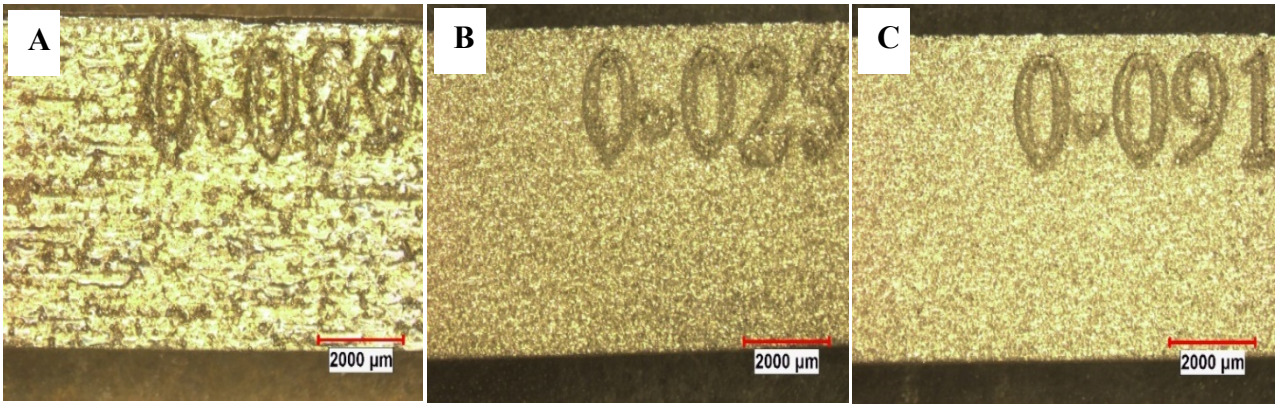


**Figure 2: Typical Optical Image of the as-built coupon after EDM removal from build platform (A) High, (B) Recommended (C) Low, all at baseline thickness of 0.889 mm**

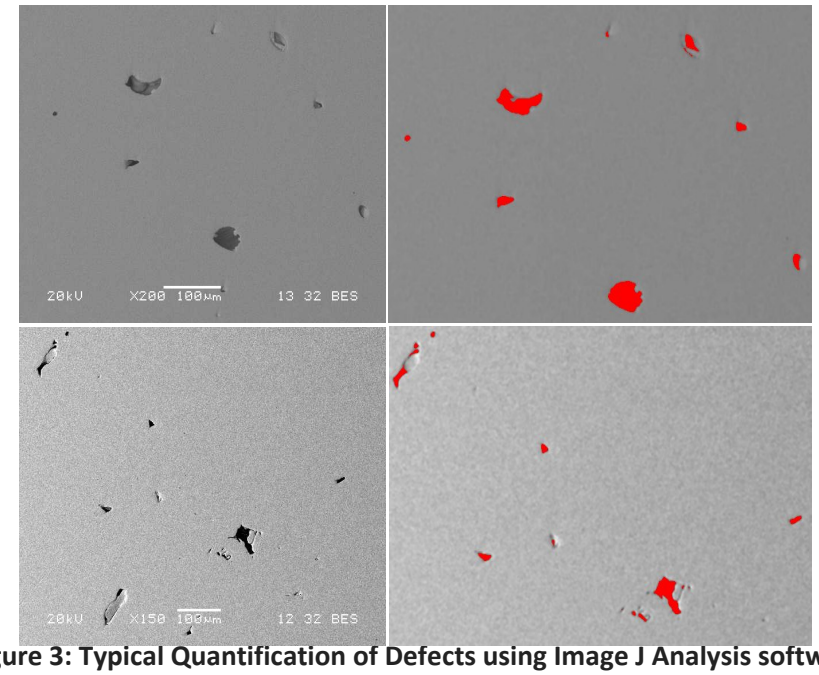


**Figure 3: Typical Quantification of Defects using Image J Analysis software**

## 3.0 RESULTS AND DISCUSSION

### 3.1 Effect of Optimization parameters on Defects and Porosity Evaluation

All the as-built and HIP coupons subjected to LPI testing passed the LPI test. Liquid penetrant inspection method was used to reveal surface discontinuities by bleed-out of a coloured or fluorescent dye from the flaw based on the ability of a liquid to be drawn into a clean surface discontinuity by capillary action (Lu and Wong, 2017; Sharratt, 2015). The advantage over an unaided visual inspection is that it makes defects easier to see by producing a flaw indication that is much larger and improves the detectability of a flaw due to the high level of contrast between the indication and the background. Although all the experimental coupons passed LPI test, nevertheless, there was a need to further investigate microstructural issues that have been previously reported in the literature (Kim *et al.*, 2017; Asala *et al.*, 2017; Zhong *et al.*, 2015; Gong *et al.*, 2015) as common to AM components. Defects such as cracks and porosity have been reported, including the influence of thickness, powder particles sizes, morphology and energy densities (Kong et al., 2007; Karapatis et al., 1999; Cleary and Sawley, 2002), however, limited information has been reported on the post-processing AM treatment effect of HIP. Therefore, selected coupons from the as-built and HIP AM coupons were section transversely to the built direction and examined using a light optical microscope (OM) and scanning electron microscope (SEM) for microstructural features. Irrespective of the energy densities process parameter used, defects ranging from porosity to incompletely melted powder were noticed at different volume fraction in all sectioned coupons (Figure 4). It is generally accepted in AM techniques that porosity can result from unstable melt pool (keyhole) formation, causing the melt pool to collapse in, and resulting in pores of inert gas or voids (Marc Saunders, 2017).

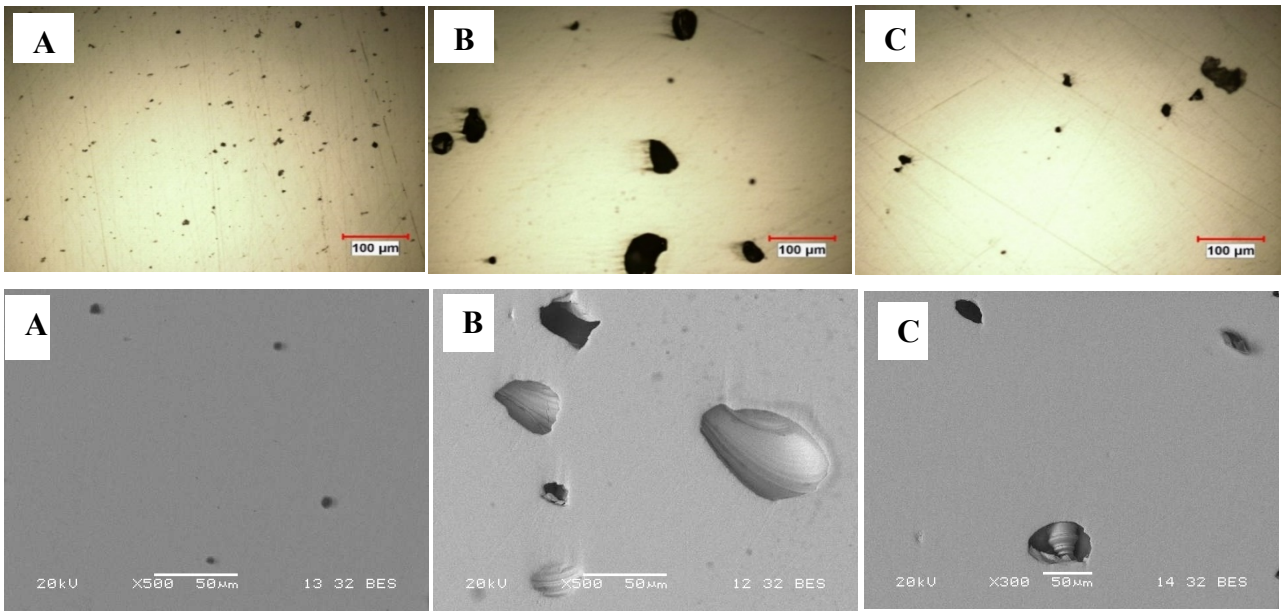


**Figure 4: Typical Optical and SEM Images of Defects in (A) Recommended (B) High and (C) Low energy density coupons, all at constant thickness 0.889 mm**

Figure 5 illustrates the combined effects of energy densities and thickness variation. Evidently, the manufacturer's recommended parameters induce the lowest % volume of defects compared to the Low ED and High ED parameters, involving processing at low speed and laser power or high speed and high laser power, respectively. In addition, variations in thicknesses of the coupons have no well-defined effect on % volume of defects observed in the study.

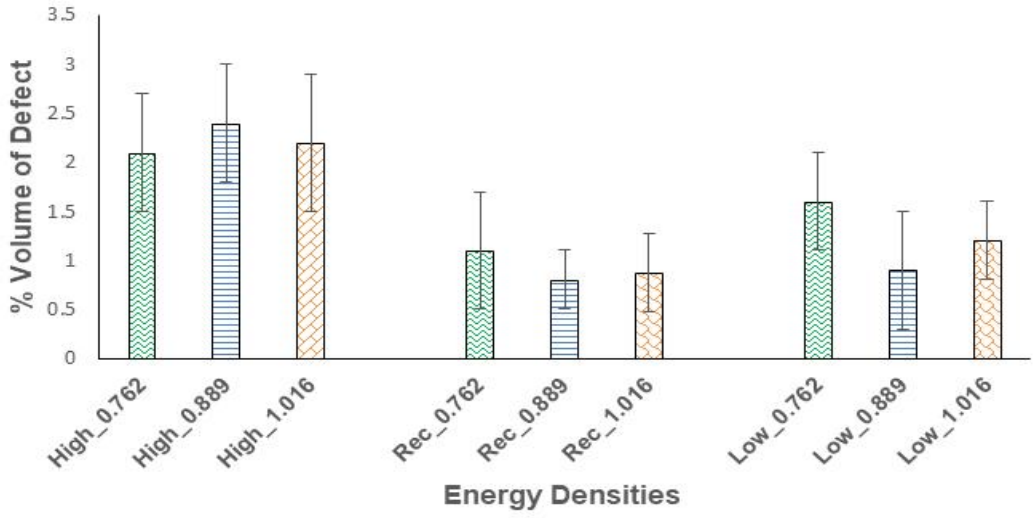


**Figure 5: Summary of the combined effect of Energy Densities and Thickness variation on % Volume of defects in Co-Cr Alloy**

Remarkably, the % volume fraction of defects reduced significantly, more so, the effect of HIP treatment appears more pronounced in the High ED and Low ED AM coupons compare to the manufacturer's recommended baseline parameters (Figures 6 and 7). While the reduction in % volume fraction of defects in the manufacturer recommended parameters is barely significant based on standard deviation, the reductions are most significant in the High ED and Low ED processing parameters, such that, the % volume fraction of defects are essentially comparable

to the values obtained in the manufacturer recommended baseline processing parameters. Hot isostatic pressing (HIP) is a manufacturing procedure used in reducing porosity of metals and increase density which ultimately improves the material's mechanical properties and workability (Atkinson and Davies, 2000). The HIP process subjects a component to both elevated temperature and isostatic gas pressure in a high-pressure containment vessel at between 50.7 MPa and 310 MPa. An inert gas at high pressure is used so that the material does not chemically react during the process as pressure is applied to the material from all directions (isostatic). During processing, soaking temperatures ranges from 482 °C to 1,320 °C depending on alloy type. The simultaneous application of heat and pressure (HIP) reduces considerably, internal voids and micro-porosity through a combination of plastic deformation, creep and diffusion bonding.

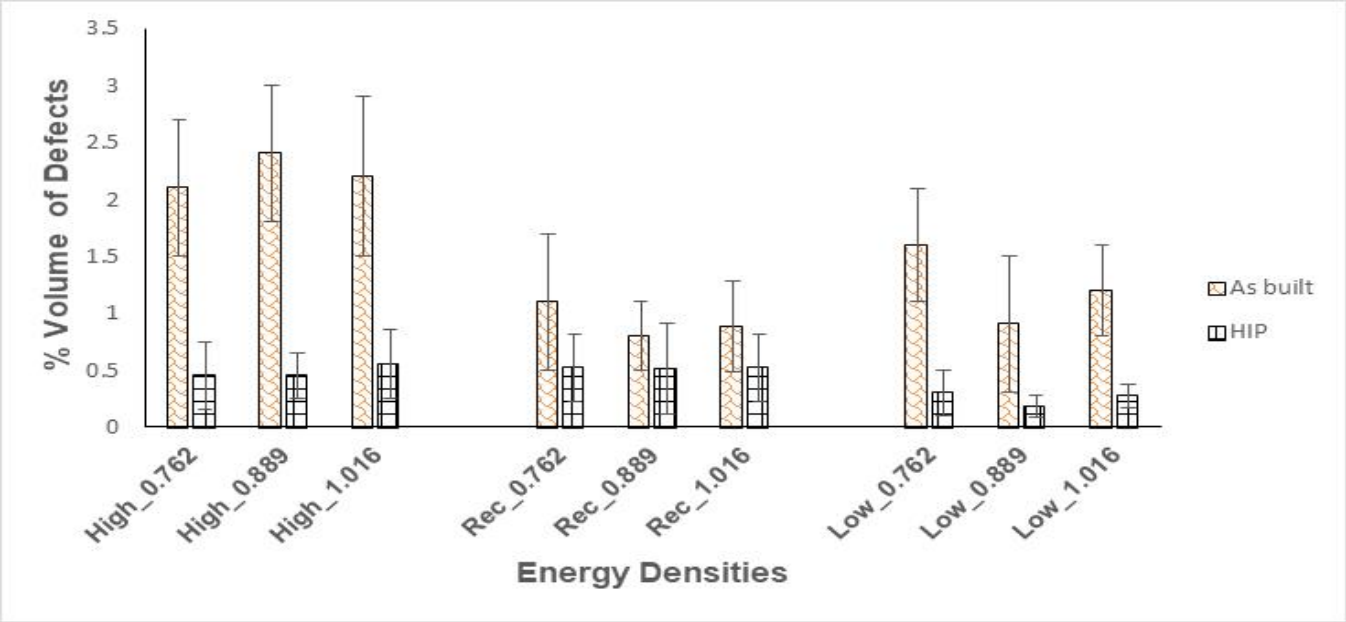


**Figure 6: Effect of HIP on % Volume Fraction of Defects**

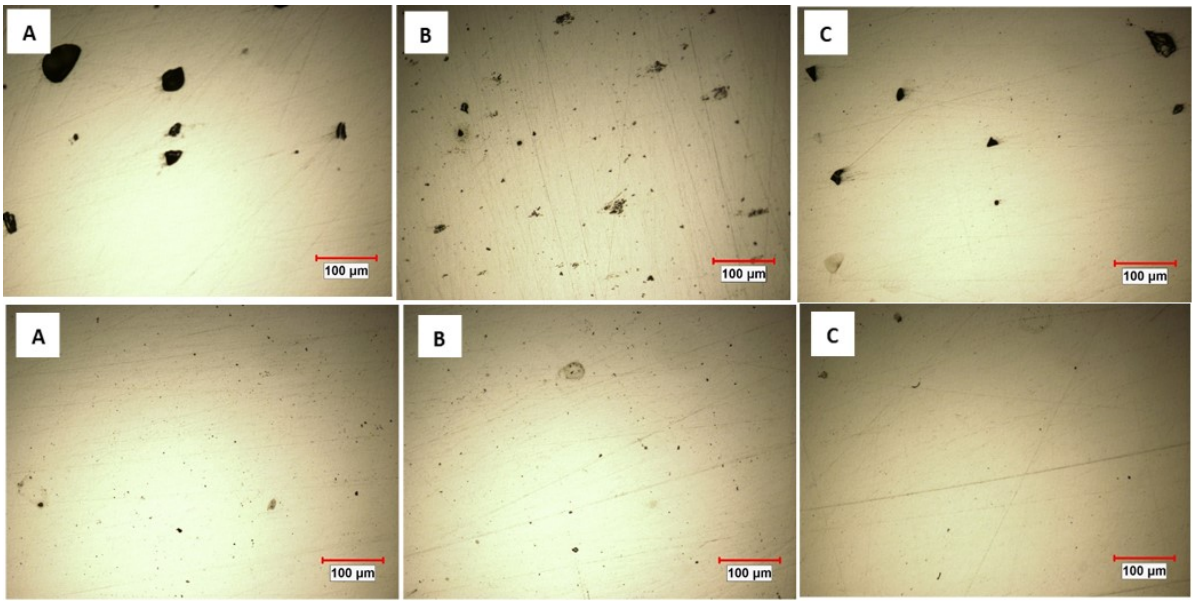


**Figure 7: As polished Optical Images of Defects in the as-built and HIP coupons at different Energy Densities in (A) High (B) Recommended and (C) Low ED, all at thickness 0.762 mm**

### 3.2 Effect of Optimization parameters on Microstructure and Hardness

The microstructure of the AM Co-Cr alloy in the as-built and HIP condition were analyzed with respects to its influence on the strength of the Co-Cr alloy. Fig. 8a-b showed the microstructures of the as-built and HIP alloy.

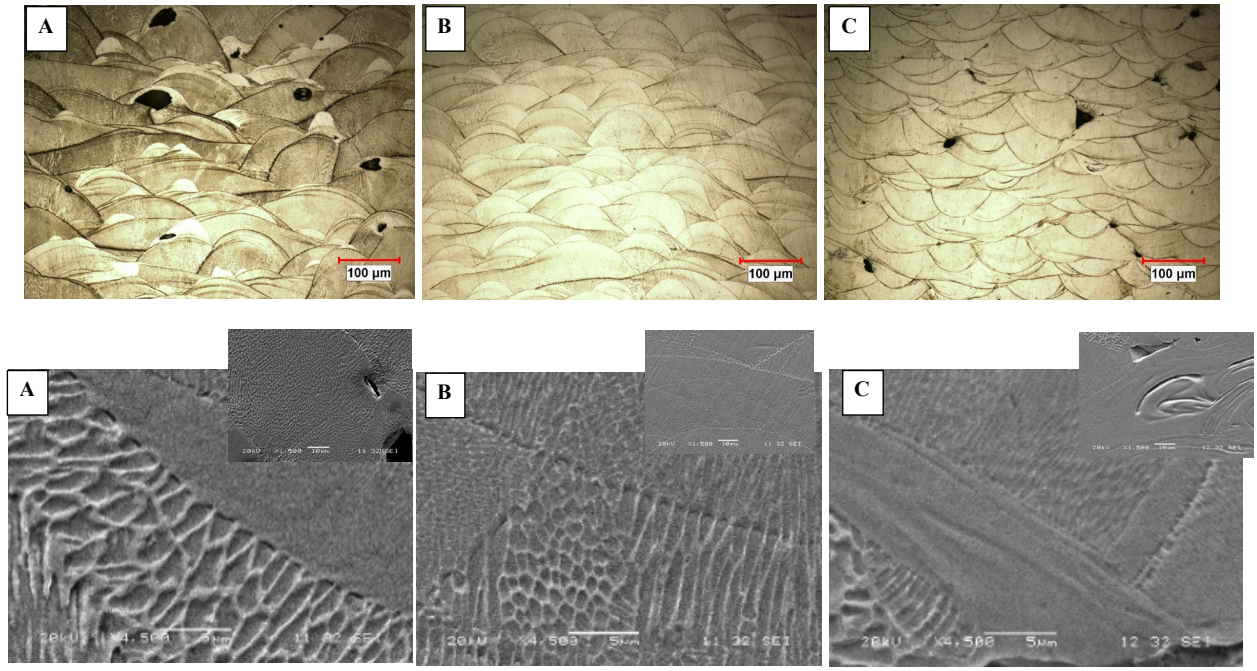


**Figure 8a: Typical Optical & SEM Images of the microstructure in as-built coupons at different Energy Densities in (A) High, (B) recommended and (C) Low ED, all at constant thickness 0.889 mm (inserts are low magnification SEM image of As-built coupons)**

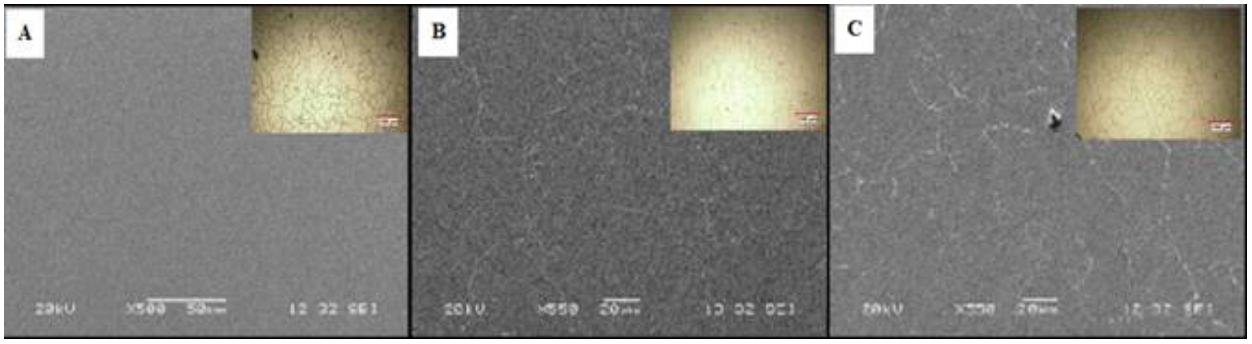


**Figure 8b: Typical Optical & SEM Images of the microstructure in HIP coupons at different Energy Densities in (A) High, (B) Recommended and (C) Low ED, all at constant thickness 0.889 mm (inserts are low magnification optical image of HIP coupons)**

The relatively small molten pool formed during PBF processing of the alloy and the consequent fast solidification in a shielding vacuum environment may be attributable to the more uniform solidification profile observed in this work. In the current study, the built direction of the different energy densities is the same (Z-direction) and as such there is no major difference in the morphology of the as-built microstructure aside the dendritic spacing, which is coarse in the HED as-built coupon and much finer in the LED (SEM insert) processing parameters while the OEM processing parameter is intermediate. Samples built with different built direction have been reported to have elongated grains along different built direction resulting in anisotropic properties (Sankaranarayanan et al., 2016). Furthermore, after the post-processing HIP treatment, the microstructure of all the coupons having different initial processing

parameters is homogenised and the grain size are comparable irrespective of the initial energy density in the as-built AM coupons.

Micro-hardness evaluation of the various energy densities processing parameters coupon showed that hardness of the High, Recommended and Low ED as-built coupons are generally comparable and after post-treatment HIP, the hardness are also comparable (Figure 9). In essence, there is no micro-hardness variation in the homogenised grain microstructure of solid solution strengthening Co-Cr alloy and as such, the mechanical properties (strength) of the AM LED as-built and HIP coupon can favourably compare and or serve as a good substitute to the manufacturer recommended baseline processing parameters properties with enhanced productivity.

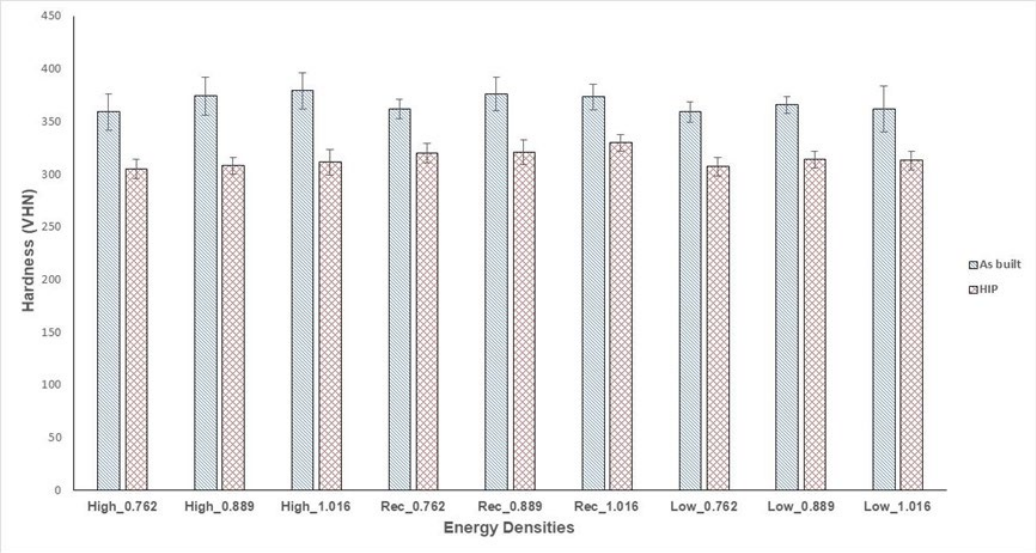


**Figure 9: shows the Micro-hardness profile of the as-built and HIP coupons at High, Recommended and Low ED, at various thicknesses.**

Surface preparation in term of roughness is the most critical step during liquid penetrant inspection (LPI) testing. As previously mentioned, LPI is a simple but reliable non-destructive test (NDT) method commonly used in ensuring/certifying the quality of AM components (Sharratt, 2015). Therefore, the effect of the different energy densities on the surface roughness of the Co-Cr alloy was evaluated in the study. Figure 10 showed the effect of the different energy densities on the surface roughness of the Co-Cr alloy in as-built and HIP condition.

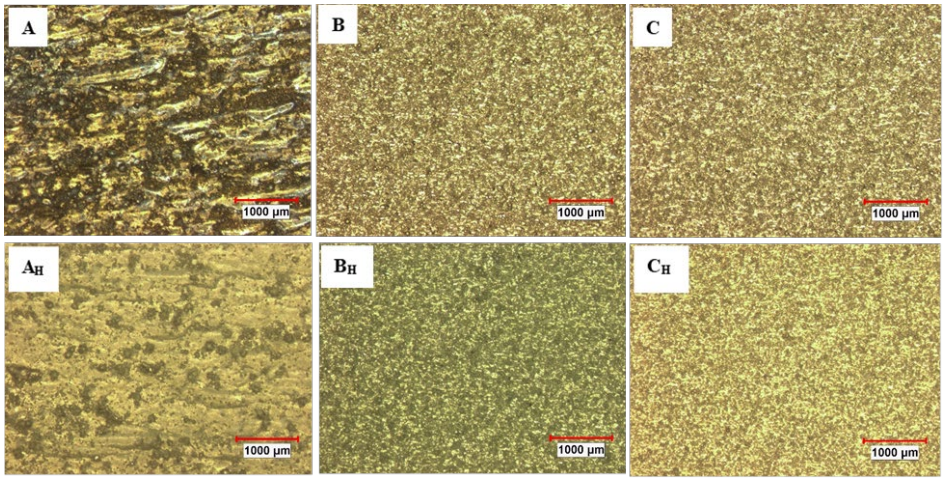


**Figure 10: Effect of Energy densities on Surface Roughness of as-built and HIP coupon in (A) High (B) Recommended, and (C) Low ED, all at baseline thickness of 0.889 mm**

Surface roughness in the High (A) is high and significantly poor compared to that in the Recommended and Low ED coupons (B & C) where the surface roughness is appreciably finer and comparable based on Light Optical Magnification Image evaluation. Post-processing treatment, HIP, of the AM coupons, moderately improved the surface roughness in the HED ($A_H$). Although HIP appears relatively effective to achieve reduced porosity, homogenized microstructure, and normalised grain size in the as-built coupons, it is however not sufficient to normalise the surface roughness in all coupons irrespective of the initial energy densities.

## 4.0. CONCLUSIONS

The effect of carefully designed process optimization parameters on AM manufactured straight wall Co-Cr Alloy has been microstructurally evaluated for defects, micro-hardness, and surface roughness. Major conclusion from the evaluation includes:

1. Although porosity is not detected by LPI in thin wall coupons produced, careful microstructural analysis of selected coupons based on process optimization parameters reveals defects of various sizes, shapes, and morphology.
2. The magnitude of Energy Densities (ED) is the most important factor that influences the % volume of defects in AM Co-Cr alloy. The baseline manufacturer recommended processing parameters induce the lowest % volume of defects in the AM Co-Cr alloy.
3. Post-processing treatment, HIP, designed to reduce porosity/defects is highly effective in reducing % volume of defects in the AM Co-Cr alloy irrespective of the initial Energy Densities in the as-built AM coupons.
4. HIP homogenised the microstructure and normalised the grain size such that they are comparable irrespective of the initial energy densities or coarse/fine dendritic structure in the as-built AM coupons, but insufficient to normalise the surface roughness in all coupons irrespective of energy densities.
5. There is no micro-hardness variation in the as-built and homogenised grain microstructure of solid solution strengthened Co-Cr alloy. Therefore, the mechanical properties (strength) of the AM LED as-built and HIP coupon compares favourably and serves as good substitute to the manufacturer recommended baseline processing parameters properties with enhanced productivity.

## 5.0 ACKNOWLEDGMENT

The authors appreciate the post-doctoral research fellowship at the University of Manitoba supported by NSERC. Materials and AM technologies provided by Precision ADM, Canada.

**REFERENCES**

Asala, G., Khan, A. K., Andersson, J., & Ojo, O. A. (2017). Microstructural analyses of ATI 718Plus® produced by wire-ARC additive manufacturing process. *Metallurgical and Materials Transactions A*, *48*(9), 4211-4228.*Atkinson, H.V., Davies, S. Fundamental aspects of hot isostatic pressing: An overview. Metallurgical and Materials Transactions. A. 31 (12): (2000) p. 2981–300.*

Baufeld, B., & Van der Biest, O. (2009). Mechanical properties of Ti-6Al-4V specimens produced by shaped metal deposition. *Science and technology of advanced materials*, *10*(1), 015008.

Choi, J., & Chang, Y. (2005). Characteristics of laser aided direct metal/material deposition process for tool steel. *International Journal of Machine Tools and Manufacture*, *45*(4-5), 597-607.

Cleary, P. W., & Sawley, M. L. (2002). DEM modelling of industrial granular flows: 3D case studies and the effect of particle shape on hopper discharge. *Applied Mathematical Modelling*, *26*(2), 89-111.

Ding, D., Pan, Z., Cuiuri, D., & Li, H. (2015). Wire-feed additive manufacturing of metal components: technologies, developments and future interests. *The International Journal of Advanced Manufacturing Technology*, *81*(1-4), 465-481.

Frazier, W. E. (2014). Metal additive manufacturing: a review. *Journal of Materials Engineering and Performance*, *23*(6), 1917-1928.

Gong, H., Rafi, K., Gu, H., Ram, G. J., Starr, T., & Stucker, B. (2015). Influence of defects on mechanical properties of Ti–6Al–4 V components produced by selective laser melting and electron beam melting. *Materials & Design*, *86*, 545-554.

Karapatis, N. P., Egger, G., Gygax, P. E., & Glardon, R. (1999). Optimization of powder layer density in selective laser sintering. In *1999 International Solid Freeform Fabrication Symposium*.

Kim, F. H., Moylan, S. P., Garboczi, E. J., & Slotwinski, J. A. (2017). Investigation of pore structure in cobalt chrome additively manufactured parts using X-ray computed tomography and three-dimensional image analysis. *Additive Manufacturing*, *17*, 23-38.

Kinsella, M. E. (2008). *Additive Manufacturing of Superalloys for Aerospace Applications (Preprint)* (No. AFRL-RX-WP-TP-2008-4318). AIR FORCE RESEARCH LAB WRIGHT-PATTERSON AFB OH MATERIALS AND MANUFACTURING DIRECTORATE.

Kong, C. Y., Carroll, P. A., Brown, P., & Scudamore, R. J. (2007, May). The effect of average powder particle size on deposition efficiency, deposit height and surface roughness in the direct metal laser deposition process. In *14th International Conference on Joining of Materials*.

Lu, Q. Y., & Wong, C. H. (2018). Additive manufacturing process monitoring and control by non-destructive testing techniques: challenges and in-process monitoring. *Virtual and physical prototyping*, *13*(2), 39-48.

Marc, S. X marks the spot - find ideal process parameters for your AM parts. https://www.linkedin.com/pulse/x-marks-spot-find-ideal-process-parameters-your-metal-marc-saunders.

Sankaranarayanan, S., Manickavasagam, K., Francis, G.C.W., Niaz, A.K. and GaryNg, K.L. (2016) Solid Freeform Fabrication*: Proceedings of the 27th Annual International Solid Freeform Fabrication Symposium* – An Additive Manufacturing Conference Reviewed Paper, 469-486.

Sharratt, B. M. (2015). Non-destructive techniques and technologies for qualification of additive manufactured parts and processes. *no. March*.

Syed, W. U. H., Pinkerton, A. J., & Li, L. (2005). A comparative study of wire feeding and powder feeding in direct diode laser deposition for rapid prototyping. *Applied surface science*, *247*(1-4), 268-276.

Thompson, S. M., Bian, L., Shamsaei, N., & Yadollahi, A. (2015). An overview of Direct Laser Deposition for additive manufacturing; Part I: Transport phenomena, modeling and diagnostics. *Additive Manufacturing*, *8*, 36-62.

Williams, S. W., Martina, F., Addison, A. C., Ding, J., Pardal, G., & Colegrove, P. (2016). Wire+ arc additive manufacturing. *Materials Science and Technology*, *32*(7), 641-647.

Xue, L. and Islam, M.U. (2006). Specialists' Meeting on Cost Effective Manufacture via Net Shape Processing (NATO/RTO AVT-139), 15:1-14.

Zhang, Y., Wei, Z., Shi, L. and Xi, M. (2008). Characterization of laser powder deposited Ti–TiC composites and functional gradient materials. *Journal of materials processing technology*. 206, 438–444.

Zhong, C., Gasser, A., Schopphoven, T., & Poprawe, R. (2015). Experimental study of porosity reduction in high deposition-rate Laser Material Deposition. *Optics & Laser Technology*, *75*, 87-92.